Self-Tuning Active Sonar Signal Processing for a Towed Hydrophone Array during a Turn

Kolja Pikora[1,2]
[1]Digital Signal Processing and System Theory
Faculty of Engineering, University of Kiel
Kiel, Germany
Email: kop@tf.uni-kiel.de /
KoljaPikora@bundeswehr.org

Frank Ehlers[2]
[2]Bundeswehr Technical Centre for Ships and Naval Weapons,
Naval Technology and Research
Research Department for Underwater Acoustics and Marine Geophysics
Kiel, Germany
Email: FrankEhlers@bundeswehr.org

***Abstract*—This paper addresses the problem of hydrophone array shape estimation of a towed array system especially during maneuvers of the tow ship. Uncertainty in the position and velocity of each sensor of the array degrades the performance of a beamformer and, hence, leads to a loss of performance for the entire data processing chain, including target tracking and (if applicable) data fusion. A self-tuning approach is developed which uses information generated by automated target tracking during the period prior to the tow ship maneuver. This information is then used to perform a sequential tracking of the antenna system during the maneuver. The antenna tracking includes the estimation of the sensor positions which is implemented as a Gaussian sum filter. This approach allows to keep the handling of multi-target situations also during the turn. First results of validating the new approach in two simulated scenarios are presented, which indicate that the approach is capable of maintaining good tracking performance during the periods of tow ship maneuvers, whilst assuming only rough knowledge about the antenna in the beamforming leads to the expected performance loss. Tracking performance is expressed in terms of probability of detection and mean squared error of the target positions. For validation purposes, the sensitivity analysis of the new approach contains Monte Carlo (MC) selections of parameters describing both the tow ship maneuver and the multi-target setup.**

I. Introduction

Sonar signal processing consists of detection, localization and tracking of targets, including data fusion in cases of spatially distributed sensors. For a given hardware (in this paper the focus is on the antenna array) sonar signal processing has to be designed to deliver optimal performance in terms of detection probability and target localization, within the constraints of real-time processing. Antenna arrays are normally towed far behind the vessel. There actual position and movement of the hydrophones are not available in global coordinates, at least not at a sufficiently high accuracy as demanded regarding the extraction of phase differences for beamforming. However, relative positions of the hydrophones to each other are well known since they correspond to the construction of the array itself. Hence, for straight line headings of the tow vessel, the assumption is that the hydrophones can be found on a line at a distance behind the tow vessel (defined by cable length and depth of the array) and with a heading indicated by a number of heading sensors built into the array. However, when the array is following a maneuver of the tow vessel, this simplified assumption turns out to be no longer valid and more sophisticated shape estimation algorithms have to be used to determine the actual positions and headings of all hydrophones and to avoid performance degradation [1]. In this paper, we investigate a self-tuning approach to estimate this positions. Clearly, more sophisticated antenna and cable motion models and more reliable built-in heading sensors could be envisioned, however the purpose of this paper is to implement and test the self-tuning approach in a high-fidelity simulation environment in order to gather first impressions on its complexity, sensitivity and performance. In other words, the focus of this paper is on the information flow from the target tracking back to the beamforming and we are interested to learn about potential performance gain and risks for failures associated to this new element added to the standard sonar signal processing chain.

Array shape estimation methods for counteracting the sensor uncertainty have been discussed extensively in the literature, and several works in the recent decades addressed this problem. The Paidoussis equation [2], [3], which describes the dynamical behavior of a thin towed array moving in water, found an application in many works. By discretization of the Paidoussis equation in space and time, a Kalman filter can be applied to measurements regarding the state of the entire sensor array [4], [5]. Other approaches use a maximum-likelihood (ML) estimate of the array resp. source parameters using a deterministic signal model [6], [7]. This method has been expanded to cases involving e. g. moving sources [8], where a ML estimator as well as a Kalman filter is used for a joint direction of arrival and array shape tracking. However, this approach suffers from multi-target situations as well as a possibly unknown number of target echoes. In this paper, the idea of using MLs and a Kalman filter for tracking the antenna itself is expanded to a parameter estimation with a Gaussian sum (GS)-filter [9] in an implementation, which provides a multi-target discrimination. It also provides additional robustness in the presence of sensor motion modeling uncertainties and reduces the dependence on potentially unreliable sensors like array heading sensors.

This work is located in a framework for self-tuning of antenna and environmental parameters. Self-tuning approaches for the signal processing are commonly used to react on changes in the physical environment of the measurement. Without adapting to these changes, the quality of contacts decreases drastically, thus the self-tuning approach can avoid the problems in tracking mentioned before. However, to initiate and guide the self-tuning process, a high confidence is mandatory that detected environmental changes are real. In this work it is

978-0-933957-43-5 ©2015 MTS

demonstrated that a self-tuning of the signal processing can be reached by passing knowledge generated by the tracking algorithm back to the beamforming process. Therefore the predicted state (in terms of the expected beam and distance) of an extracted and confirmed track (i.e. associated with a high confidence level in the tracking algorithm) is tuning the parameters of the beamforming algorithm. This newly developed processing step has the capability to estimate several parameters of the towed antenna like heading and turn rate, according to the information coming from the tracking algorithm. In simulations, we demonstrate that by this self-tuning the tracking performance increases, compared to results without self-tuning, in terms of a higher track probability of detection and lower mean squared error of the targets positions. The core idea for the development of the self-adapting beamforming step is to combine the following criteria for estimating the array shape parameters during the entire turning phase of the tow vessel: (i) maximization of the signal to noise ratio (SNR) of the contact in the confirmed track that has triggered the self-tuning process in the expected beam and distance, (ii) minimizing the covariance of resulting contact of the confirmed track after the tracking step, (iii) the ability for multi-target discrimination (where available and automatically detected).
The proposed algorithm is tested in Monte Carlo simulations within an underwater simulation framework which provides the hydrophone signal data for bistatic scenarios. As a target tracking scenario, a bistatic active sonar setup is chosen, in which a stationary omni directional transmitter operates in the low frequency domain and a tow platform makes 180° curves with different curvature radii.
The paper is organized as follows. In Section II the antenna signal model used in this paper is presented, afterwards Section III gives an overview about the signal processing chain for active sonar. Section IV introduces the self-tuning approach, Section V shows simulation setups and results. A conclusion and an outlook are given in Section VI

II. ANTENNA SIGNAL MODEL

We assume a twin line hydrophone array, whose left-right ambiguity is perfectly resolved within the signal processing. Hence, for simplification the following explanations concern a single line array with $\mathrm{N^h}$ hydrophones. Let $\mathbf{x}_\mathrm{r} = \left(x_\mathrm{r}, y_\mathrm{r}, \dot{x}_\mathrm{r}, \dot{y}_\mathrm{r}, \theta_\mathrm{r}, \psi_\mathrm{r}\right)^\mathrm{T}$ be the state vector of the tow ship and $\mathbf{x}_\mathrm{r}^\mathrm{h} = \left(x_\mathrm{r}^\mathrm{h}, y_\mathrm{r}^\mathrm{h}, \dot{x}_\mathrm{r}^\mathrm{h}, \dot{y}_\mathrm{r}^\mathrm{h}, \theta_\mathrm{r}^\mathrm{h}, \psi_\mathrm{r}^\mathrm{h}\right)^\mathrm{T}$ the state of the hth hydrophone in the towed array, where $h = 1, \ldots, \mathrm{N^h}$, x and y are the Cartesian position, $\dot{x}$ and $\dot{y}$ the Cartesian velocity, θ is the heading relative to north (with positive degree clockwise on starboard and negative degrees counterclockwise on portside) and $\psi = \dot{\theta}$ is the turn rate. Furthermore let the reference hydrophone be denoted by $\mathbf{x}_\mathrm{r}^1$. The received signal $u_\mathrm{r}^\mathrm{h}(t)$ at the output of the hth hydrophone can be described by

$$u_\mathrm{r}^\mathrm{h}(t) = \sum_{n=1}^{\mathrm{N^n}} u_\mathrm{s}\Big(t - \tau_\mathrm{n} - \tau_\mathrm{h}(\phi_\mathrm{n})\Big) + \upsilon_\mathrm{h}(t), \tag{1}$$

which includes $\mathrm{N^n}$ replicates of the transmitted signal $u_\mathrm{s}(t)$, delayed by a transmission time τ_n and a time delay τ_h relative to the reference hydrophone, which depends on the incoming angle ϕ_n of the nth reflection. $\upsilon_\mathrm{h}(t)$ is an additive Gaussian noise term. In general, the time delay $\tau_\mathrm{h}(\phi)$ can be expressed as

$$\tau_\mathrm{h}(\phi) = \frac{\left(x_\mathrm{r}^\mathrm{h} - x_\mathrm{r}^1\right)\cdot \sin(\phi) + \left(y_\mathrm{r}^\mathrm{h} - y_\mathrm{r}^1\right)\cdot\cos(\phi)}{c}, \tag{2}$$

where c is the speed of sound. The calculation of the Cartesian positions of the hydrophones depends on the movement of the tow ship. For a linear movement of the ship it is assumed, that the towed hydrophone array follows a linear motion model and the same heading as the ship, which means $\theta_\mathrm{r} = \theta_\mathrm{r}^1$, but positioned behind the tow ship. Hence the position of the reference hydrophone is

$$\begin{aligned} x_\mathrm{r}^1 &= x_\mathrm{r} - \delta_\mathrm{C}\sin(\theta_\mathrm{r}) \\ y_\mathrm{r}^1 &= y_\mathrm{r} - \delta_\mathrm{C}\cos(\theta_\mathrm{r}) \end{aligned}$$

and of the other hydrophones

$$x_\mathrm{r}^\mathrm{h} = x_\mathrm{r}^1 - h\cdot\delta_\mathrm{h}\cdot\sin(\theta_\mathrm{r}) \tag{3}$$
$$y_\mathrm{r}^\mathrm{h} = y_\mathrm{r}^1 - h\cdot\delta_\mathrm{h}\cdot\cos(\theta_\mathrm{r}), \tag{4}$$

where δ_C is the length of the tow cable and δ_h is the distance between two hydrophones. In a turn we assume a nearly constant turn rate model [10], where the Cartesian coordinates depend on a turn rate of the reference hydrophone.

$$x_\mathrm{r}^\mathrm{h} = x_\mathrm{r}^1 - h\cdot\delta_\mathrm{h}\left[\mathrm{CW}\cos\theta_\mathrm{r}^1 + \mathrm{SW}\sin\theta_\mathrm{r}^1\right] \tag{5}$$
$$y_\mathrm{r}^\mathrm{h} = y_\mathrm{r}^1 - h\cdot\delta_\mathrm{h}\left[\mathrm{SW}\cos\theta_\mathrm{r}^1 - \mathrm{CW}\sin\theta_\mathrm{r}^1\right], \tag{6}$$

with

$$\mathrm{SW} = \frac{\sin\left(\psi_\mathrm{r}^1 T_\mathrm{P}\right)}{\psi_\mathrm{r}^1 T_\mathrm{P}}, \quad \mathrm{CW} = \frac{1-\cos\left(\psi_\mathrm{r}^1 T_\mathrm{P}\right)}{\psi_\mathrm{r}^1 T_\mathrm{P}},$$

where T_P is the ping period. Please note on the one hand, that (5) and (6) correspond to (3) and (4) if $\psi_\mathrm{r}^1 = 0$, and on the other hand, that $\theta_\mathrm{r}^\mathrm{h} \neq \theta_\mathrm{r}$ when $\psi_\mathrm{r}^1 \neq 0$. The model just described uses two parameters to describe the antenna shape during the turn: the heading θ_r^1 as well as the turn rate ψ_r^1 of the reference hydrophone. An exact knowledge of these parameters is fundamental for generating contacts from the received data as it will be described in Section III.

III. ACTIVE SONAR SIGNAL PROCESSING CHAIN

The active sonar signal processing contains two central steps. At first, contacts of potential targets as well as reflections from clutter are extracted from the hydrophone signals. Afterwards these contacts are processed by a sequential tracking approach for creating tracks of potential targets. The contact generation and the complete sequence for target tracking are shown in Fig. 1 and Fig. 2.

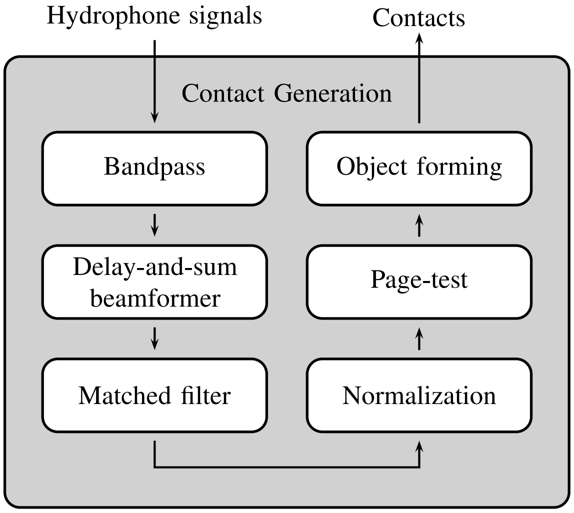

Fig. 1: Active sonar signal processing chain for generating contacts from the hydrophone signals.

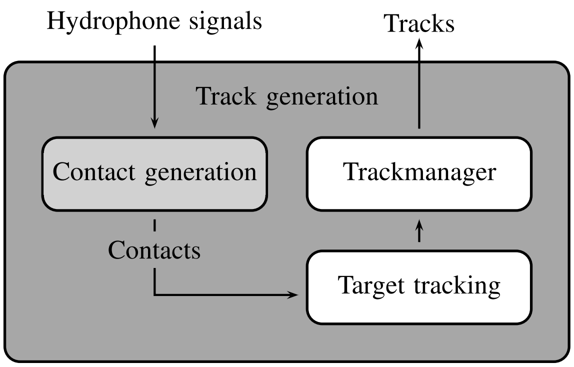

Fig. 2: Complete sequence for target tracking in one timestep, containing the contact generation as well as the tracking procedure.

A. Contact Generation

At first the hydrophone signals are band pass filtered and afterwards processed by a delay and sum beamformer (DSBF), which performs a spatial filtering of the data by steering through the angles of interest. The following components in the contact generation are a matched filter for increasing the SNR of the echoes by correlating the received signals with the transmitted pulse, a normalizer to deal with time invariance of reverberation and noise, a Page-test detector [11] and an object forming step. In the following we focus on the beamforming step, which is mainly influenced by the turn parameters. The signal in beam Θ

$$u_\Theta\big(t\big) = \sum_{h=1}^{\mathrm{N}^{\mathrm{h}}} \omega^*\big(h, \Theta\big) u_{\mathrm{r}}^{\mathrm{h}}\big(t\big), \tag{7}$$

is calculated by the multiplication of the hydrophone signals with beamformer weights

$$\omega\big(h, \Theta\big) = \exp\big(i2\pi f \tau_{\mathrm{h}}\big(\Theta\big)\big), \tag{8}$$

with the signal frequency f. For simplification, we consider here a narrowband beamformer and ignore a shading of the beamformer weights. In the case, when $\tau_{\mathrm{h}}\big(\Theta\big) = \tau_{\mathrm{h}}\big(\phi_{\mathrm{n}}\big)$ for all $h = 1, \ldots, \mathrm{N}^{\mathrm{h}}$ the reflected signal of reflection n appears with the highest possible SNR in the beam signal. Vice versa, a loss of SNR occurs, if the time delays do not exactly match each other. Moreover it can happen, that a reflection does not appear in the beam where it originated if the heading of the reference hydrophone does not match the heading used for calculation of the time delays $\tau_{\mathrm{h}}\big(\Theta\big)$. Accordingly an uncertainty on the parameters to describe the antenna shape during the turn results in a wrong calculation of the phase delay between the hydrophones, and thus leads to an incorrect detection of a reflection regarding the position.

For this work two different hyperbolic frequency modulated (HFM) signals, one with an increasing frequency gradient (HFM^+) the other with a decreasing frequency gradient (HFM^-), are transmitted. Thus contacts are generated for each signal type $\mathbf{S} \in \{+, -\}$ in a semi-coherent signal processing chain [12]. Each chain at time k creates a contact set containing $\mathrm{N}^{\mathrm{z}}_{\mathrm{k},\mathbf{S}}$ measurement vectors $\mathbf{Z}_{\mathrm{k},\mathbf{S}} = \Big\{\boldsymbol{z}^1_{\mathrm{k},\mathbf{S}}, \ldots, \boldsymbol{z}^{\mathrm{N}^{\mathrm{z}}_{\mathrm{k},\mathbf{S}}}_{\mathrm{k},\mathbf{S}}\Big\}$, each representing a detected echo. A measurement vector is defined by

$$\boldsymbol{z}_{\mathbf{S}} = \big(\tau_{\mathbf{S}}, \varphi_{\mathbf{S}}\big)^{\mathrm{T}}, \tag{9}$$

where τ is the time of arrival, which is the bistatic range divided by the speed of sound (which is assumed to be constant over range and time), φ is the azimuth measurement and $\big(\cdot\big)^{\mathrm{T}}$ means transposed. By fusion of the contacts of the different chains one can obtain contacts with an additional range-rate approximation of the echo

$$\boldsymbol{z}_{\mathrm{f}} = \big(\tau_{\mathrm{f}}, \varphi_{\mathrm{f}}, \dot{\tau}_{\mathrm{f}}\big)^{\mathrm{T}}, \tag{10}$$

with $\dot{\tau}$ being the bistatic range-rate, which is proportional to the Doppler (see [12], [13] for further details). The connection between the position of a target (target state) and a measurement is formulated in the measurement equation. With $\mathbf{x}_{\mathrm{q}} = \big(x_{\mathrm{q}}, y_{\mathrm{q}}\big)^{\mathrm{T}}$ being the position of an echo and $\mathbf{x}_{\mathrm{s}} = \big(x_{\mathrm{s}}, y_{\mathrm{s}}\big)^{\mathrm{T}}$ the source position, the measurements defined in (9) resp. (10) can be expressed as

$$\begin{aligned}
\tau &= \frac{|\mathbf{x}_{\mathrm{q}} - \mathbf{x}_{\mathrm{s}}| + |\mathbf{x}_{\mathrm{q}} - \mathbf{x}^1_{\mathrm{r}}|}{c} \\
\varphi &= \arctan\left(\frac{x_{\mathrm{q}} - x^1_{\mathrm{r}}}{y_{\mathrm{q}} - y^1_{\mathrm{r}}}\right) - \theta^1_{\mathrm{r}} \\
\dot{\tau} &= \frac{\delta\tau}{\delta t} c,
\end{aligned} \tag{11}$$

where $|\cdots|$ denotes the Euclidian norm.

B. Track Generation

In this work the target tracking step is applied with a cardinalized probability hypothesis density (CPHD) filter [14], [15] which is a further development of the probability hypothesis density (PHD) filter. In general, the PHD filter alleviates the computational intractability of the multi-target Bayes filter by approximating the density of the multi-target state by the propagation of the intensity (expected value) of the target states. Furthermore the filter provides an estimate of the number of targets in the field of view (FoV), although this value is susceptible to high occurrence of clutter. The CPHD filter handles this problem by jointly propagating the intensity as well as the cardinality distribution (the probability distribution of the number of targets). In Gaussian mixture implementation (Gaussian Mixture Cardinalized PHD (GMCPHD) [16], [17]) the intensity of target states is approximated by a sum of Gaussian components, which include mean $\mathbf{m}$, covariance $\mathbf{P}$ and weight w

$$D_{\mathrm{k}}(x) = \sum_{j=1}^{\mathrm{N}_{\mathrm{k}}^{\mathrm{j}}} w_{\mathrm{k}}^{\mathrm{j}} \mathcal{N}\Big(x; \mathbf{m}_{\mathrm{k}}^{\mathrm{j}}, \mathbf{P}_{\mathrm{k}}^{\mathrm{j}}\Big). \tag{12}$$

There D_{k} is the intensity at time step k, $\mathrm{N}_{\mathrm{k}}^{\mathrm{j}}$ is the number of Gaussian components and $\mathcal{N}(\,\cdot\,)$ describes the multivariate Gaussian function. The filter propagates the intensity of the multi-target state in time by a prediction and a subsequent update of the intensity (see [16] or [18] for details and [19] for implementation issues).

IV. Self-Tuning Approach

We introduce a self-tuning approach for mitigating the uncertainty in array shape during a turn of a ship. The self-tuning approach investigated is based on passing knowledge generated by the target tracking algorithm back to the beamforming process in that moment when the targets localization quality is decreasing or the turn of the tow ship starts. Based on this knowledge the antenna turn parameters are estimated in an antenna tracking step, which includes a ML estimation implemented in a GS filter. Fig. 3 gives an schematic overview of the entire self-tuning recursion.

A. Track/Maneuver Analysis

At the beginning, the self-tuning procedure decides on the basis of two independent criteria, if a self-tuning of the antenna trajectory is necessary:

- As a measurement of the quality of extracted tracks the first criterion describes the occurrence of track performance loss (TPL). Because the state covariance matrix is directly used for calculating the posterior weights of the Gaussian mixture (GM)-components, we can simply compare the posterior weights at time k and $k-1$. We define here
$$\frac{w_{\mathrm{k|k}}}{w_{\mathrm{k-1}}} < \delta^{\mathrm{TPL}}, \quad 0 < \delta^{\mathrm{TPL}} \leq 1 \tag{13}$$
as the condition for a TPL.
- The second criterion turn of ship (TOS) focuses on the movement of the tow ship. Considering the time t we define
$$t^{\mathrm{TOS}} - \delta^{\mathrm{TOS}} \leq t \leq t^{\mathrm{TOS}} + \delta^{\mathrm{TOS}}, \tag{14}$$
as the condition for a TOS. In (14) t^{TOS} is the time when the tow ship starts a turn and $\delta^{\mathrm{TOS}} \geq 0$ is a time offset. We assume here, that the tow ship is starting a turn immediately when the transmitter starts a ping. The parameter δ^{TOS} should be adjusted considering the length of the cable from ship to array taking into account, that the cable follows the ship in the turn, close to the position where the ship started the turn.

B. Antenna Tracking

In the antenna tracking, possible reference hydrophone positions including several sets for the antenna motion model parameters (turn rate and heading) are predicted and afterwards updated by using contacts, which are generated separately for each predicted position. The model for the state of the reference hydrophone $\boldsymbol{\zeta}_{\mathrm{k}}$ that we address is given by

$$\begin{aligned} \boldsymbol{\zeta}_{\mathrm{k}} &= f(\boldsymbol{\zeta}_{\mathrm{k-1}}) + \nu_{\mathrm{k}} \\ \boldsymbol{z}_{\mathrm{k}} &= h(\boldsymbol{\zeta}_{\mathrm{k}}) + \epsilon_{\mathrm{k}}, \end{aligned} \tag{15}$$

where ν_{k} and ϵ_{k} are assumed to be Gaussian noise. The state of the reference hydrophone at time k is defined as

$$\boldsymbol{\zeta}_{\mathrm{k}} = \big(x_\zeta, y_\zeta, \dot{x}_\zeta, \dot{y}_\zeta, \theta_\zeta, \psi_\zeta\big)^{\mathrm{T}}, \tag{16}$$

where x_ζ and y_ζ are the Cartesian position of the reference hydrophone, $\dot{x}_\zeta$ and $\dot{y}_\zeta$ are the velocity in direction x and y,

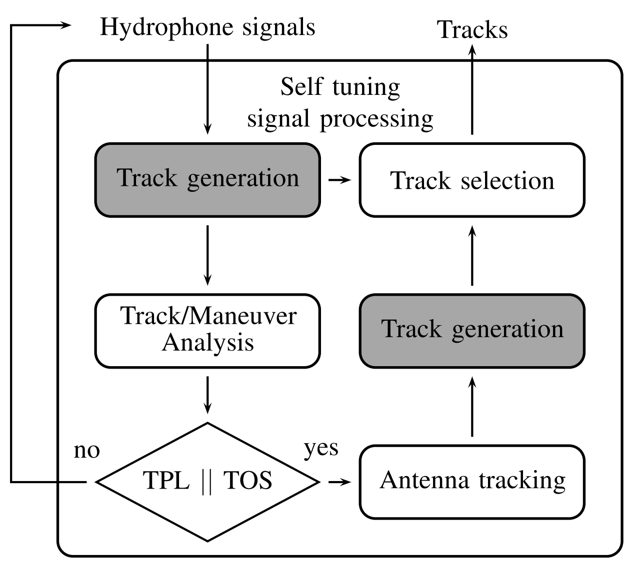

Fig. 3: Schematic self-tuning signal processing. TPL: Track performance loss, TOS: Turn of ship

θ_ζ is the heading relative to north and ψ_ζ is the turn rate. The uncertainty associated with the state vector $\boldsymbol{\zeta}_\mathrm{k}$ is characterized by the probability density function (pdf) $p(\boldsymbol{\zeta}_\mathrm{k})$ and the task is to find the posterior distribution $p(\boldsymbol{\zeta}_\mathrm{k}|\mathbf{Z}_\mathrm{k})$ of $\boldsymbol{\zeta}_\mathrm{k}$ given a contact set $\mathbf{Z}_\mathrm{k}$. By using a GS-filter [9] the distribution of the reference hydrophone density can be modeled as a finite sum of Gaussian pdfs

$$p(\boldsymbol{\zeta}_\mathrm{k}|\mathbf{Z}_\mathrm{k}) = \sum_{j=1}^{\mathrm{N}_\mathrm{k}^\mathrm{j}} w_{\zeta,\mathrm{k}}^\mathrm{j} \mathcal{N}\Big(\zeta; \mathbf{m}_{\zeta,\mathrm{k}}^\mathrm{j}, \mathbf{P}_{\zeta,\mathrm{k}}^\mathrm{j}\Big), \tag{17}$$

where $\mathbf{m}_{\zeta,\mathrm{k}}^\mathrm{j}$ and $\mathbf{P}_{\zeta,\mathrm{k}}^\mathrm{j}$ represent the conditional mean and covariance of the jth component of the Gaussian pdf with respect to the measurements and $w_{\zeta,\mathrm{k}}^\mathrm{j}$ denotes the amplitude. With this definition it is possible to predict and update the means and covariances of the GS by using an extended Kalman filter. Please note at this point that $\boldsymbol{\zeta}_\mathrm{k}$ is an approximation of the reference hydrophone state as member of a multivariate Gaussian distribution, while $\mathbf{x}_\mathrm{r}^1$ illustrates the real position of the reference hydrophone within the antenna motion model.
Moreover notice the difference between (12) and (17): While (12) describes an intensity and thus the expected value of a multi target density, (17) describes the density itself. In contrast to the weights of the Gaussian components in the PHD the amplitudes of the Gaussian components in (17) underlie a constraint regarding positivity and normalization of the pdf

$$\sum_{j=1}^{\mathrm{N}_\mathrm{k}^\mathrm{j}} w_{\zeta,\mathrm{k}}^\mathrm{j} = 1, \quad w_{\zeta,\mathrm{k}}^\mathrm{j} \geq 0 \tag{18}$$

1) Prediction: For the prediction of the GS model is used which consists of the surviving GM components as well as new GM components regarding a certain birth model. Assuming there exists a GS $G_{\mathrm{k}-1}(\boldsymbol{\zeta}) = \hat{p}(\boldsymbol{\zeta}_{\mathrm{k}-1}|\mathbf{Z}_{\mathrm{k}-1})$ at time step $k-1$ as an approximation of the posterior distribution of the reference hydrophone state, the surviving part is calculated by

$$G_{\mathrm{S,k|k-1}}(\boldsymbol{\zeta}) = \sum_{j=1}^{\mathrm{N}_{\mathrm{S,k-1}}^\mathrm{j}} w_{\mathrm{S,k|k-1}}^\mathrm{j} \mathcal{N}\Big(\boldsymbol{\zeta}; \mathbf{m}_{\mathrm{S,k|k-1}}^\mathrm{j}, \mathbf{P}_{\mathrm{S,k|k-1}}^\mathrm{j}\Big), \tag{19}$$

where

$$\begin{aligned} \mathbf{m}_{\mathrm{S,k|k-1}}^\mathrm{j} &= \mathbf{F}_{\mathrm{k}-1}\mathbf{m}_{\zeta,\mathrm{k}-1}^\mathrm{j} \\ \mathbf{P}_{\mathrm{S,k|k-1}}^\mathrm{j} &= \mathbf{F}_{\mathrm{k}-1}\mathbf{P}_{\zeta,\mathrm{k}-1}^\mathrm{j}\mathbf{F}_{\mathrm{k}-1}^\mathrm{T} + \mathbf{Q}_{\mathrm{k}-1} \\ w_{\mathrm{S,k|k-1}}^\mathrm{j} &= w_{\zeta,\mathrm{k}-1}^\mathrm{j} \end{aligned} \tag{20}$$

are the prior mean, covariance and weight of component j. $\mathbf{F}_{\mathrm{k}-1}$ describes the transition matrix, $\mathbf{Q}_{\mathrm{k}-1}$ is the process noise matrix.
The GS of the new born components $G_{\mathrm{B,k}}(\boldsymbol{\zeta})$ is independent of the measurements and is designed to cover an area where the antenna is expected to be (with constraints on speed and turn rate):

- The magnitude of the velocity of a new born a priori component of the reference hydrophone $v_{\zeta,\mathrm{B,k|k-1}}$ does not increase compared to the last time step and does not decrease more than v_l due to a turn. Thus
$$v_{\zeta,\mathrm{k}-1} \geq v_{\zeta,\mathrm{B,k|k-1}} \geq v_{\zeta,\mathrm{k}-1} - v_\mathrm{l} \tag{21}$$
- The antenna will perform a turn with maximal α degrees per second. Thus the prior turn rate $\psi_{\zeta,\mathrm{B,k|k-1}}$ of a newly born component of the reference hydrophone will be
$$\psi_{\zeta,\mathrm{k}-1} - \alpha T_\mathrm{P} \leq \psi_{\zeta,\mathrm{B,k|k-1}} \leq \psi_{\zeta,\mathrm{k}-1} + \alpha T_\mathrm{P} \tag{22}$$
- The area which is covered by the surviving components should not be covered by any newly born component.

The resulting area is afterwards approximated with $\mathrm{N}_{\mathrm{k|k-1}}^{\mathrm{GM}}$ GMs using an expectation maximization (EM) algorithm from [20], which ensures that the complete area is nearly uniformly covered by this set of Gaussian mixtures. The complete prior GS is described by

$$G_{\mathrm{k|k-1}}(\boldsymbol{\zeta}) = G_{\mathrm{S,k|k-1}}(\boldsymbol{\zeta}) + G_{\mathrm{B,k}}(\boldsymbol{\zeta}), \tag{23}$$

$$= \sum_{j=1}^{\mathrm{N}_{\mathrm{k|k-1}}^\mathrm{j}} w_{\zeta,\mathrm{k|k-1}}^\mathrm{j} \mathcal{N}\Big(\boldsymbol{\zeta}; \mathbf{m}_{\zeta,\mathrm{k|k-1}}^\mathrm{j}, \mathbf{P}_{\zeta,\mathrm{k|k-1}}^\mathrm{j}\Big) \tag{24}$$

and contains a total number of $\mathrm{N}_{\mathrm{k|k-1}}^\mathrm{j} = \mathrm{N}_{\mathrm{k|k-1}}^{\mathrm{GM}} + \mathrm{N}_{\mathrm{S,k-1}}$ Gaussian components which represent possible prior positions for the reference hydrophone position.

2) Update: Since the bistatic state of transmitter, receiver and targets defines the observation of the antenna, the semi-coherent contact generation has to be performed for each predicted reference hydrophone position $\mathbf{m}_{\zeta,\mathrm{k|k-1}}^\mathrm{j}$ individually. To avoid high computational load, contacts are generated only in areas where extracted target tracks are predicted. This simplification can be understood as rough gating step before the signal processing.
Assume a number of $\mathrm{N}^\mathcal{T}$ tracks with prior state $\mathbf{x}_{\mathrm{k|k-1}}^\mathrm{n} = \left(x_{\mathrm{k|k-1}}^\mathrm{n}, y_{\mathrm{k|k-1}}^\mathrm{n}, \dot{x}_{\mathrm{k|k-1}}^\mathrm{n}, \dot{y}_{\mathrm{k|k-1}}^\mathrm{n}\right)^\mathrm{T}$ and covariance $\mathbf{P}_{\mathrm{k|k-1}}^\mathrm{n}$, $n = 1, \ldots, \mathrm{N}^\mathcal{T}$, which are extracted by the target tracker and thus reliable. The contact sets for each signal type generated in the rectangle area surrounding the covariance of track n for the prior reference hydrophone j are $\mathbf{Z}_\mathbf{S}^{\mathrm{j,n}} = \left\{\boldsymbol{z}_{\mathbf{S}\mathrm{j,n}}^1, \ldots, \boldsymbol{z}_{\mathbf{S},\mathrm{j,n}}^{\mathrm{N}_{\mathbf{S},\mathrm{j,n}}^\mathrm{z}}\right\}$. The contact $\boldsymbol{z}_{\mathbf{S},\mathrm{j}}^\mathrm{z}$ is defined to be any contact in the contact set $\mathbf{Z}_\mathbf{S}^\mathrm{j} = \mathbf{Z}_\mathbf{S}^{\mathrm{j},1} \cup \ldots \cup \mathbf{Z}_\mathbf{S}^{\mathrm{j},\mathrm{N}^\mathcal{T}}$, which contains all contacts of one signal processing chain for a priori reference hydrophone j. The update of the jth component is performed by calculating the likelihood for each multi-target association of contacts in $\mathbf{Z}_+^\mathrm{j}$, $\mathbf{Z}_-^\mathrm{j}$ and tracks. Due to the fact, that the number of targets is rather small and the number of contacts is kept small due to the rough gating, the number of necessary associations is obviously limited. In the following, the contact set $\mathbf{Z}^\mathrm{j}$ contains contacts $\boldsymbol{z}_\mathrm{j}^\mathrm{z}$, created from the fusion of all combinations of contacts in $\mathbf{Z}_+^\mathrm{j}$ and $\mathbf{Z}_-^\mathrm{j}$. The update procedure for the posterior weights is as follows:

1. Transform the prior estimate of the reference hydrophone $\mathbf{m}^{\mathrm{j}}_{\zeta,\mathrm{k|k-1}}$ in the measurement space using the measurement function h which can be derived from (11)
$$\hat{\boldsymbol{z}}_{\mathrm{j,n}} = h\big(\mathbf{m}^{\mathrm{j}}_{\zeta,\mathrm{k|k-1}}, \mathbf{x}^{\mathrm{n}}_{\mathrm{k|k-1}}, \mathbf{x}_{\mathrm{s}}\big). \tag{25}$$
2. Calculate the measurement residual covariance (also called innovation covariance) $\hat{\boldsymbol{S}}^{\mathrm{z}}_{\mathrm{j}}$ by
$$\hat{\boldsymbol{S}}^{\mathrm{z}}_{\mathrm{j}} = \mathbf{H}_{\mathrm{j,n}} \mathbf{P}^{\mathrm{j}}_{\zeta,\mathrm{k|k-1}} \big(\mathbf{H}_{\mathrm{j,n}}\big)^{\mathrm{T}} + \mathbf{R}^{\mathrm{z}}_{\mathrm{j}}, \tag{26}$$
where $\mathbf{R}^{\mathrm{z}}_{\mathrm{j}}$ is the covariance of contact $\boldsymbol{z}^{\mathrm{z}}_{\mathrm{j}} \in \mathbf{Z}^{\mathrm{j}}$.
$$\mathbf{H}_{\mathrm{j,n}} = \frac{\partial h}{\partial \mathbf{x}_{\mathrm{r}}}\Big|_{\mathbf{x}_{\mathrm{r}} = \mathbf{m}^{\mathrm{j}}_{\zeta,\mathrm{k|k-1}}} \tag{27}$$
is the Jacobian matrix of the measurement function.
3. Determine the likelihood for associating contact $\boldsymbol{z}^{\mathrm{z}}_{\zeta,\mathrm{j}}$ to track n
$$\ell^{\mathrm{z}}_{\mathrm{j,n}} = \mathcal{N}\big(\boldsymbol{z}^{\mathrm{z}}_{\mathrm{j}}; \hat{\boldsymbol{z}}_{\mathrm{j,n}}, \hat{\boldsymbol{S}}^{\mathrm{z}}_{\mathrm{j,n}}\big). \tag{28}$$
4. Define hypotheses $\mathcal{H}^{\mathrm{a}}_{\mathrm{j}}$ for all possible associations of measurements in contact set $\mathbf{Z}^{\mathrm{j}}$ to target tracks, where $a = 1, \ldots, \mathrm{N}^{\mathrm{a}}_{\mathrm{j}}$ and $\mathrm{N}^{\mathrm{a}}_{\mathrm{j}}$ is the total number of associations and each hypothesis is an unique association generated by $\mathbf{m}^{\mathrm{j}}_{\zeta,\mathrm{k|k-1}}, \boldsymbol{z}^{\mathrm{z}}_{\mathrm{j}} \in \mathbf{A}^{\mathrm{a}}_{\mathrm{j}}$ and $\mathbf{x}^{\mathrm{n}}_{\mathrm{k|k-1}}$. With $\mathbf{A}^{\mathrm{a}}_{\mathrm{j}}$ being the set of measurements, associated with a track, the multi-target likelihood $\mathcal{L}\big(\mathcal{H}^{\mathrm{a}}_{\mathrm{j}}\big)$ is calculated by
$$\mathcal{L}\big(\mathcal{H}^{\mathrm{a}}_{\mathrm{j}}\big) = \big(1 - p_{\mathrm{d}}\big)^{\mathrm{N}^{\varnothing}} \big(p_{\mathrm{d}}\big)^{\mathrm{N}^{\mathrm{d}}} \big(\kappa\big)^{\mathrm{N}^{\varnothing}} \prod_{\boldsymbol{z}^{\mathrm{z}}_{\mathrm{j}} \in \mathbf{A}^{\mathrm{a}}_{\mathrm{j}}} \ell^{\mathrm{z}}_{\mathrm{j,n}}, \tag{29}$$
where $\mathrm{N}^{\varnothing}$ is the number of tracks without associated contact, N^{d} is the number of tracks with associated contact and κ is the density of clutter. In particular the number of associations for one predicted reference hydrophone position is
$$\mathrm{N}^{\mathrm{a}}_{\mathrm{j}} = 1 + \frac{\big(1 + |\mathbf{Z}^{\mathrm{j}}|\big)!}{\big(1 + |\mathbf{Z}^{\mathrm{j}}| - \mathrm{N}^{\mathcal{T}}\big)!}, \tag{30}$$
including hypotheses for missing a detection of a track.

The posterior weights of the reference hydrophones are calculated by normalizing the multi-target likelihoods and considering the prior reference hydrophone weight:
$$w^{\mathrm{j}}_{\mathrm{a,k|k}} = w^{\mathrm{j}}_{\mathrm{k|k-1}} \cdot \frac{\mathcal{L}\big(\mathcal{H}^{\mathrm{a}}_{\mathrm{j}}\big)}{\sum_{a=1}^{\mathrm{N}^{\mathrm{a}}} \mathcal{L}\big(\mathcal{H}^{\mathrm{a}}_{\mathrm{j}}\big)}. \tag{31}$$

After executing this procedure for each predicted reference hydrophone the total number of associations is
$$\mathrm{N}^{\mathrm{a}} = \sum_{j=1}^{\mathrm{N}^{\mathrm{j}}_{\mathrm{k|k-1}}} \mathrm{N}^{\mathrm{a}}_{\mathrm{j}},$$
and the set of all hypotheses is $\mathcal{H}^{\mathrm{a}} = \Big\{\mathcal{H}^{\mathrm{a}}_{1}, \ldots, \mathcal{H}^{\mathrm{a}}_{\mathrm{N}^{\mathrm{j}}_{\mathrm{k|k-1}}}\Big\}$. To reduce the number of posterior hypotheses (and thus the computational load) a pruning step chooses only the N^{b} hypotheses with the highest weights $w^{\mathrm{j}}_{\mathrm{a,k|k}}$, namely $\mathcal{H}^{\mathrm{b}}$. Let $\mathcal{H}^{\mathrm{b}}$ be generated by $\mathbf{m}^{\mathrm{b}}_{\zeta,\mathrm{k|k-1}}$ and $\mathbf{A}^{\mathrm{b}}_{\mathrm{j}}$ containing associations of $\mathbf{x}^{\mathrm{n}}_{\mathrm{k|k-1}}$ and $\boldsymbol{z}^{\mathrm{z}}_{\mathrm{b}} \in \mathbf{Z}^{\mathrm{b}}$. The posterior state of the reference hydrophone is calculated by recursively updating the prior state with the contacts $\boldsymbol{z}^{\mathrm{z}}_{\mathrm{b}} \in \mathbf{Z}^{\mathrm{b}}$ with reference to $\mathbf{x}^{\mathrm{n}}_{\mathrm{k|k-1}}$ using the extended transformation:
$$\begin{aligned} \mathbf{m}^{\mathrm{b}}_{\zeta,\mathrm{k|k}} &= \mathbf{m}^{\mathrm{b}}_{\zeta,\mathrm{k|k-1}} + \mathbf{K}^{\mathrm{b}}\big(\boldsymbol{z}^{\mathrm{b}}_{\mathrm{z}} - \hat{\boldsymbol{z}}_{\mathrm{b,n}}\big) \\ \mathbf{P}^{\mathrm{b}}_{\zeta,\mathrm{k|k}} &= \mathbf{P}^{\mathrm{b}}_{\zeta,\mathrm{k|k-1}} - \mathbf{K}^{\mathrm{b}} \mathbf{H}_{\mathrm{b,n}} \mathbf{P}^{\mathrm{b}}_{\zeta,\mathrm{k|k-1}}, \end{aligned} \tag{32}$$
with the Kalman gain
$$\mathbf{K}^{\mathrm{b}} = \mathbf{P}^{\mathrm{b}}_{\zeta,\mathrm{k|k-1}} \mathbf{H}_{\mathrm{b,n}} \big(\big(\mathbf{H}_{\mathrm{b,n}}\big)^{\mathrm{T}} \mathbf{P}^{\mathrm{b}}_{\zeta,\mathrm{k|k-1}} \mathbf{H}_{\mathrm{b,n}} + \mathbf{R}^{\mathrm{z}}_{\mathrm{b}}\big)^{-1}. \tag{33}$$

Please note, that $\mathbf{m}^{\mathrm{b}}_{\zeta,\mathrm{k|k-1}} = \mathbf{m}^{\mathrm{b}}_{\zeta,\mathrm{k|k}}$ and $\mathbf{P}^{\mathrm{b}}_{\zeta,\mathrm{k|k-1}} = \mathbf{P}^{\mathrm{b}}_{\zeta,\mathrm{k|k}}$ after each time calculating (32) and (33) recursively.

The resulting GS at time step k is described by the posterior GS
$$G_{\mathrm{k|k}}(\zeta) = \sum_{b=1}^{\mathrm{N}^{\mathrm{b}}} w^{\mathrm{b}}_{\mathrm{k|k}} \mathcal{N}\Big(\boldsymbol{\zeta}; \mathbf{m}^{\mathrm{b}}_{\zeta,\mathrm{k|k}}, \mathbf{P}^{\mathrm{b}}_{\zeta,\mathrm{k|k}}\Big). \tag{34}$$

The component with the highest weight, namely $w^{\mathrm{b,max}}_{\mathrm{k|k}}$ (which can be understood as ML estimator) is afterwards taken as the new state of the reference hydrophone and thus used for the following contact and target track generation for the complete FoV.

C. Track Selection

After performing a target track generation with the best component of the antenna density, it is decided whether the bistatic geometry including the estimated antenna position leads to better target tracking results than before. Let $\mathbf{x}^{\mathrm{n}}_{\mathrm{k|k}}$ resp. $\mathbf{x}^{\mathrm{n,b}}_{\mathrm{k|k}}$ be the posterior target states generated in bistatic geometries without resp. with the self-tuning procedure for target n. Consequently the self-tuned parameters are taken as the new ones if $w^{\mathrm{n,b}}_{\mathrm{k|k}} / w^{\mathrm{n}}_{\mathrm{k|k}} \geq 1$ for each target. Otherwise the old parameters are kept for the next time step.

V. Tracking Simulations and Results

The results are created using a previously verified and applied hydrophone signal simulator [21], conceptionally similar to the simulator described in [22]. It provides hydrophone signals for a given parametrization of a scenario. This parametrization contains e.g. bistatic geometries, waveform details and underwater channel properties.
For the benchmark of the results we use the track performance metrics which were developed for comparability of tracking results within the Multistatic Tracking Working Group (MSTWG) [23].

A. Simulation Setup

Three different scenarios have been designed: In Scenario 1 two moving targets and two unknown fixed clutter points are simulated in the FoV of one bistatic source receiver pair. Each $60\,\mathrm{s}$ ($T_{\mathrm{P}} = 60\,\mathrm{s}$) the source transmits a pulse consisting of two HFM waveforms, one with increasing frequency gradient, the other with decreasing frequency gradient (see [12] for details). The receiver track consists of 2 legs and a turn. Each leg takes $8\,\mathrm{min}$. The length of the turn varies and depends on the turn radii: In Scenario 1a the tow ships performs a turn of $3\,\mathrm{min}$ and $\approx 800\,\mathrm{m}$ radius, in Scenario 1b a turn of $2\,\mathrm{min}$ and $\approx 500\,\mathrm{m}$ radius. The setups of Scenario 1a and 1b are shown in Fig. 4. For analyzing the capability for multi-target discrimination of the algorithm, Scenario 2 includes two moving targets and two unknown fixed clutter points as well and two unknown fixed clutter points which lay close to the trajectory of target 2. The bistatic geometry as well as the movement of the receiver remain the same as in Scenarios 1a and 1b. The setup of Scenario 2 is shown in Fig. 4.
In all scenarios we use the parameter set shown in Tab. I:

B. Monte Carlo Setup

If not specified otherwise we perform 20 MC runs for each simulation setup. The trajectories of the tow ship remain the same for each MC run and it is assumed, that the speed of the ship is not decreasing during a turn. The trajectory of the towed array is changing for each run and underlies a decreasing velocity during the turn. Hence, it is assumed that the ground truth of the towed array is indeed initialized with the correct position but is subsequently unknown. The random parameter for the MC runs is the initial turn rate $\psi_{\mathrm{r}}^{1'}$ of the towed array at time step $k_{\mathrm{first}}^{\mathrm{TOS}}-1$, which is assumed to be equal the outgoing

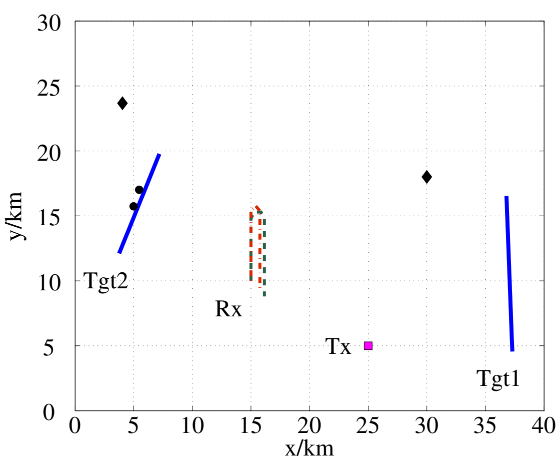

Fig. 4: Setup of Scenarios 1a, 1b and 2. Scenarios 1a and 1b include a bistatic geometry with receiver (Rx, 1a: Green, dashed line, 1b: Red, dash-dot line), source (Tx, magenta, square), targets (Tgt1 and Tgt2, blue lines) and fixed clutter points (black, diamonds). Scenario 2 includes a bistatic geometry with receiver (Rx, Green, dashed line), source (Tx, magenta, square), targets (Tgt1 and Tgt2, blue lines) and fixed clutter points (black, diamonds and black, dots)

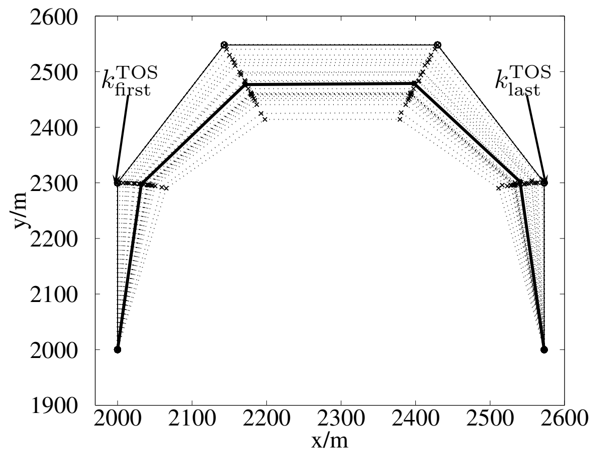

Fig. 5: Example trajectories for 20 turns of the towing ship showing the trajectory of the towing ship (thin solid line), the mean of resulting towed array trajectories (thick solid line) and the simulated towed array trajectories (dotted lines).

turn rate at time step $k_{\mathrm{last}}^{\mathrm{TOS}}+1$. $\psi_{\mathrm{r}}^{1'}$ is Gaussian distributed with mean $0.25\,^{\circ}/\mathrm{s}$ and standard deviation $0.1\,^{\circ}/\mathrm{s}$. Fig. 5 shows examples for the resulting towed array trajectories.
For each MC run the hydrophone signals are generated. This set of signals serves as input to three different implementations of the self-tuning algorithm. The implementations differ in how much prior knowledge is available to the tracking and estimation steps the self-tuning algorithm consists of and if the self-tuning step is activated: (i) The turn is exactly known and self-tuning is disabled(in the following called: setup TEK), (ii) the mean of the turn in all MC runs is known and self-tuning is disabled (setup TMK, this implementation can be interpreted as the case where knowledge about the turn is roughly available), (iii) the turn parameters are completely unknown and estimated by the self-tuning approach (setup TAT).
The purpose of this analysis is to gather insight on how capable

Twin-line hydrophone array	
Number of hydrophones in one line	$\mathrm{N^h} = 128$
Distance between towing ship and reference hydrophone	$\delta_{\mathrm{C}} = 1000\,\mathrm{m}$
Distance between two hydrophones	$\delta_{\mathrm{h}} = 0.24\,\mathrm{m}$
Self-tuning step	
Track/Maneuver Analysis:	
Relative loss of weight as condition for TPL (13)	$\delta^{\mathrm{TPL}} = 0.6$
Look ahead time for a turn detection (TOS, (14))	$\delta^{\mathrm{TOS}} = 120\,\mathrm{s}$
Prediction:	
Number of GMs for approximation of the predicted area where the antenna is expected to be	$\mathrm{N^{GM}} = 24$
Maximum loss of velocity during turn (21)	$v_{\mathrm{l}} = 4\,\mathrm{m/s}$
Maximum turn rate allowed in a turn (22)	$\alpha = 1\,\mathrm{deg}\,/\mathrm{s}$
Update:	
Probability of detection of a target in multi-target likelihood calculation (29)	$p_{\mathrm{d}} = 0.8$
Number of GMs to be kept before update	$\mathrm{N^b} = 3$

TABLE I: Parametrization of the self-tuning procedure the tracking and estimation steps are. A benchmarking with an algorithm that stops generating contact data during a turn would obviously lead to lower track probability of detection (TPD)s and higher localization errors. We will show in the next sub-section that the self-tuning algorithm is capable of maintaining contact generation and tracking accordingly also during a turn.

C. Tracking Results

For calculating the mean track-localization error (MTLE) and TPD only the two moving targets are assumed to be known. The unknown fixed targets do not appear in the calculation for MTLE and TPD. For comparability and clarity we split the trajectory of the towed array in three phases: Before the turn, during the turn and after the turn.
Fig. 8 and Fig. 11 show the MTLE and TPD for Scenario 1a. The results are summarized in the following.

- Before the turn the MTLE for all algorithmic implementations are identical. The TPD stays at 1.0 for all algorithmic implementations. At the time step before the turn starts, TAT detects the turn and starts the self-tuning which leads to a low localization error compared to TEK and TMK.
- During the turn, the targets pass the endfire regions of the antenna. Thus, the MTLE has to be higher than before or after the turn. During the turn TAT gives a better approximation of the antenna trajectory than TMK, resulting in a smaller MTLE. TAT is able to keep the TPD constant at 1.0 whilst the TMK implementation is not.
- After the turn TEK and TMK localize the targets with nearly the same MTLE. TAT detects the end of the turn but exits the turn at another position than the real turn exits. Hence the target tracks are spatially shifted, resulting in a higher MTLE. Note, that according to the description of the self-tuning algorithm (Fig. 3) the self-tuning is not switched on after the turn, hence it cannot continue correcting the trajectory of the reference hydrophone. In TMK the targets are again extracted, thus the TPD rises up to 1.0 again.

Fig. 9 and Fig. 12 show the MTLE and TPD for Scenario 1b. The results can be described by the same effects like in Scenario 1a.
Fig. 10 and Fig. 13 show the MTLE and TPD for Scenario 2. The results are summarized in the following.

- Before the turn the MTLE and TPD for the three algorithmic implementations behave like in Scenario 1a and 1b.
- During the turn the three algorithmic implementations show a similar MTLE. The main error originates again from the endfire region of the hydrophone array where the probability to detect a target decreases. An additional effect is located in the target tracking step where the multi-target situation leads to false associations of contacts generated by the unknown fixed clutter points and the moving targets. As a consequence the tracks of the moving targets might be deleted. The TPD again is decreasing only for TMK.
- After the turn the behavior of the three algorithmic implementations is similar to Scenarios 1a and 1b.

The effect of a lower MTLE for setup TMK in Scenario 2 compared with setup TMK in Scenarios 1a and 1b may be explained by the contacts of the fixed objects laying in the confidence ellipse of the moving target and consequently associations of contacts originated by the fixed objects with the moving target. Note, that the target tracking algorithms implemented here do not contain any association steps which would allow for keeping the fixed objects staying at the same position before, during and after the turn.
The root mean squared error (RMSE) of the reference hydrophone position, as well as the RMSE of the parameters estimated in the self-tuning procedure for Scenarios 1a and 2 are shown in Fig. 6 and Fig. 7. Before the turn starts, the RMSE of the reference hydrophone as well as the RMSE of both parameters of the antenna shape model is zero, because no TOS or TPL occurred and hence no self-tuning was done. Through the optimal initialization the prediction in the further time steps is optimal, too. At the beginning of the turn the RMSE of the reference hydrophone position is increasing but stays below $100\,\mathrm{m}$ in both scenarios. Obviously the multi-target case does not negatively effect the reference hydrophone estimation. Instead it is an improvement to use more fixed clutter points for estimation of the antenna state.

VI. Conclusion and Outlook

In this paper we focused on the estimation of the hydrophone array shape during a turn by self-tuning the parameters of an antenna movement model. We found that an estimation of the turn parameters array heading and turn rate can be implemented as a GS tracking filter for the antenna respectively the reference hydrophone in the antenna itself. We applied the self-tuning procedure on several scenarios, containing different curve radii of a towed array as well as multi-target situations, and compared the tracking results of the new approach with cases where prior knowledge about the array parameters is exactly resp. roughly available. Within the approach we made some constraints regarding the initial position of the hydrophone array which is assumed to be known, and regarding unknown fixed clutter objects in the surveillance which has to be detected by the target tracker until the turn starts. However, the purpose of this paper is, to gather first impressions on the implementation of a self-tuning approach which uses an information flow from the target tracking back to the beamforming. Therefore, these constraints are deemed to be a reasonable balance between algorithmic complexity and more realistic modeling.
Compared to the case where the parameters of the array are roughly known, the loss of TPD during the turn can be mitigated by using the self-tuning approach. Moreover the targets of interest are estimated with a smaller localization error if the self-tuning procedure is used. The approach can handle multi-target situations by calculating multi-target likelihood to track associations.
In future work, the estimation of the antenna state needs to be improved, in particular the elimination of the positioning error after the turn is mandatory. Furthermore, extensions of the algorithm by adding information from potentially very unreliable heading sensors filtered within the Kalman filter procedure and

by adding multistatic data fusion seem to be viable. Special attention should be given to the effect of a bias in the initial position of the reference hydrophone which could lead to a combination of the algorithm for system parameter estimations [21] with the current self-tuning approach presented in this paper.

ACKNOWLEDGMENT

The authors are grateful to Dr. Martina Brötje for valuable discussions about the topic of parameter estimation.

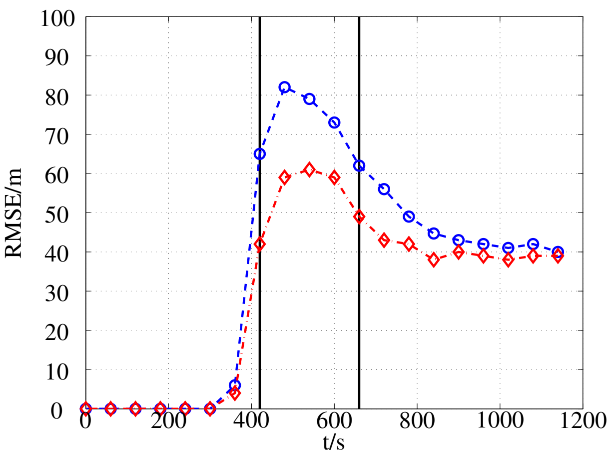

Fig. 6: Root mean squared error of the reference hydrophone. Scenario 1a: Blue, circles, Scenario 2: Red, diamonds

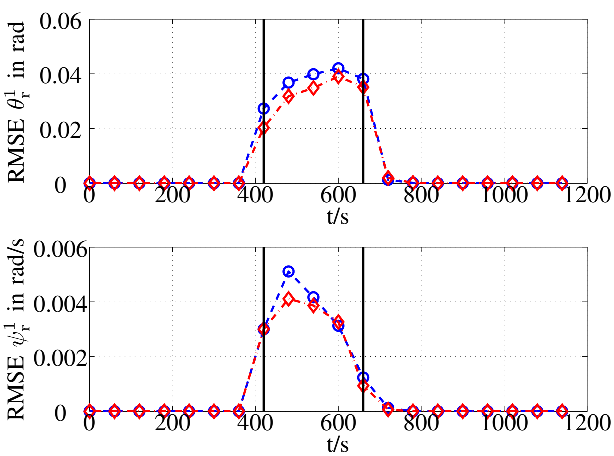

Fig. 7: Root mean squared errors of the critical parameters heading (top) and turnrate (below) of the hydrophone array. Scenario 1a: Blue, circles, Scenario 2: Red, diamonds

REFERENCES

[1] W. Hodgkiss, "The effects of array shape perturbation on beamforming and passive ranging," *IEEE Journal of Oceanic Engineering*, vol. OE-8, no. 3, pp. 120–130, July 1983.

[2] M.P.Paidoussis, "Dynamics of flexible slender cylinder in axial flow; part i theory," *Journal of Fluid Mechanics*, vol. 26, pp. 717–736, 1966.

[3] ——, "Dynamics of flexible slender cylinder in axial flow; part ii experiment," *Journal of Fluid Mechanics*, vol. 26, pp. 737–751, 1966.

[4] J. Riley and D. Gray, "Towed array shape estimation using kalman filters-experimental investigations," *IEEE Journal of Oceanic Engineering*, vol. 18, no. 4, pp. 572–581, Oct 1993.

[5] N. Nikitakos, A. Leros, and S. Katsikas, "Towed array shape estimation using multimodel partitioning filters," *IEEE Journal of Oceanic Engineering*, vol. 23, no. 4, pp. 380–384, Oct 1998.

[6] A. Weiss and B. Friedlander, "Array shape calibration using sources in unknown locations-a maximum likelihood approach," in *1988 International Conference on Acoustics, Speech, and Signal Processing, 1988. ICASSP-88.*, Apr 1988, pp. 2670–2673 vol.5.

[7] ——, "Array shape calibration using eigenstructure methods," in *Signals, Systems and Computers, 1989. Twenty-Third Asilomar Conference on*, vol. 2, 1989, pp. 925–929.

[8] J. Goldberg, A. Perez-Neira, and M. A. Lagunas, "Joint direction-of-arrival and array shape tracking for multiple moving targets," in *1997 IEEE International Conference on Acoustics, Speech, and Signal Processing, 1997. ICASSP-97.*, vol. 1, Apr 1997, pp. 511–514 vol.1.

[9] D. Alspach and S. H.W., "Nonlinear bayesian estimation using gaussian sum approximations," *IEEE Transactions on Automatic Control*, vol. 17, no. 4, pp. 439–448, Aug 1972.

[10] R. P. S. Blackman, *Design and Analysis of Modern Tracking Systems*. Artech House, 1999.

[11] D. Abraham and P. Willett, "Active sonar detection in shallow water using the page test," *IEEE Journal of Oceanic Engineering*, vol. 27, no. 1, pp. 35–46, Jan 2002.

[12] K. Pikora and F. Ehlers, "Tracking Performance Loss due to False Associations of Contacts from Semi-Coherent Signal Processing Chains," in *2014 17th International Conference on Information Fusion (FUSION)*, July 2014.

[13] X. Song, P. Willett, and S. Zhou, "Range Bias Modeling for Hyperbolic-Frequency-Modulated Waveforms in Target Tracking," *Oceanic Engineering, IEEE Journal of*, vol. 37, no. 4, pp. 670–679, 2012.

[14] R. Mahler, "Approximate multisensor CPHD and PHD filters," in *2010 13th Conference on Information Fusion (FUSION)*, 2010, pp. 1–8.

[15] ——, "PHD filters of higher order in target number," *Aerospace and Electronic Systems, IEEE Transactions on*, vol. 43, no. 4, pp. 1523 –1543, october 2007.

[16] B.-N. V. Ba-Tuong Vo and A. Cantoni, "Analytic Implementations of the Cardinalized Probability Hypothesis Density Filter," *IEEE Transactions on Signal Processing*, vol. 55, no. 7, July 2007.

[17] H. Zhang, Z. Jing, and S. Hu, "Gaussian mixture CPHD filter with gating technique," *Signal Process.*, vol. 89, no. 8, pp. 1521–1530, Aug. 2009.

[18] M. Ulmke, O. Erdinc, and P. Willett, "Gaussian mixture cardinalized PHD filter for ground moving target tracking," in *Information Fusion, 2007 10th International Conference on*, july 2007, pp. 1 –8.

[19] K. Pikora and F. Ehlers, "Analysis of the FKIE Passive Radar Data Set with GMPHD and GMCPHD," in *2013 16th International Conference on Information Fusion (FUSION)*, 2013.

[20] N. Vlassis and L. Aristidis, "A Greedy EM Algorithm for Gaussian Mixture Learning," *Neural Process. Lett.*, vol. 15, no. 1, pp. 77–87, feb 2002.

[21] M. Broetje and K. Pikora, "Parameter estimation for multistatic active sonar using extended fixed points," in *2015 18th International Conference on Information Fusion (FUSION)*, 2015.

[22] P. de Theije and H. Groen, "Multistatic Sonar Simulations with SIMONA," in *Information Fusion, 2006 9th International Conference on*, July 2006, pp. 1–6.

[23] S. Coraluppi, D. Grimmett, and P. de Theije, "Benchmark Evaluation of Multistatic Trackers," in *Information Fusion, 2006 9th International Conference on*, july 2006, pp. 1 –7.

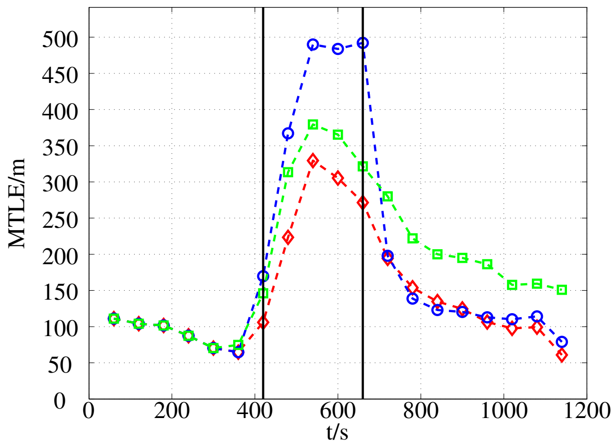

Fig. 8: Mean Track Localization Error of targets in Scenario 1a. Turn from 420 s to 640 s. TEK (red, diamonds), TMK (blue, circles), TAT (green, squares)

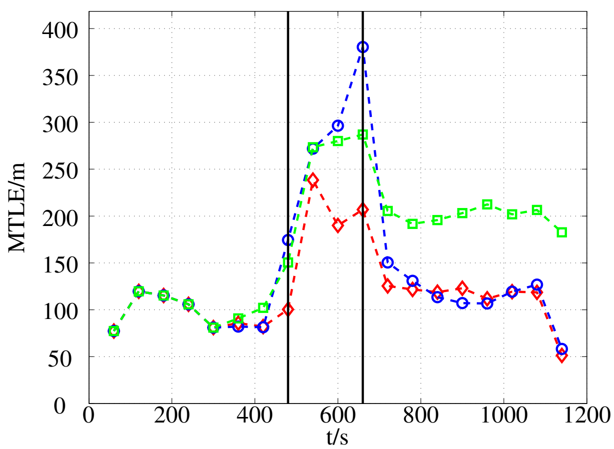

Fig. 9: Mean Track Localization Error of targets in Scenario 1b. Turn from 480 s to 640 s. TEK (red, diamonds), TMK (blue, circles), TAT (green, squares)

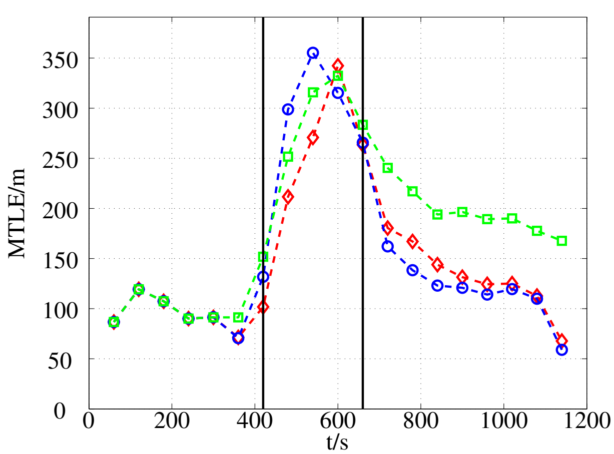

Fig. 10: Mean Track Localization Error of targets in Scenario 2. Turn from 420 s to 640 s. TEK (red, diamonds), TMK (blue, circles), TAT (green, squares)

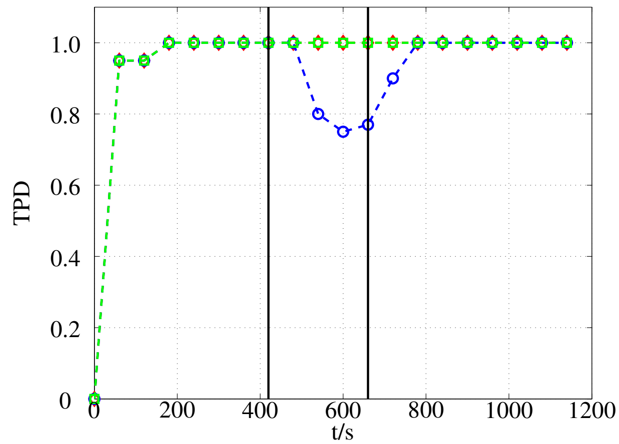

Fig. 11: Track probability of detection of targets in Scenario 1a. Turn from 420 s to 640 s. TEK (red, diamonds), TMK (blue, circles), TAT (green, squares)

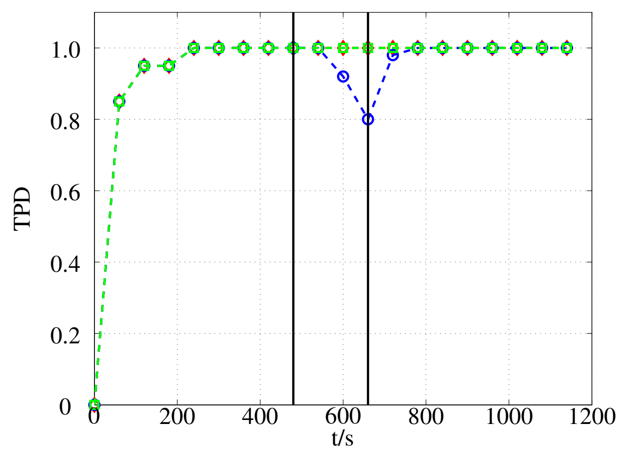

Fig. 12: Track probability of detection of targets in Scenario 1b. Turn from 480 s to 640 s. TEK (red, diamonds), TMK (blue, circles), TAT (green, squares)

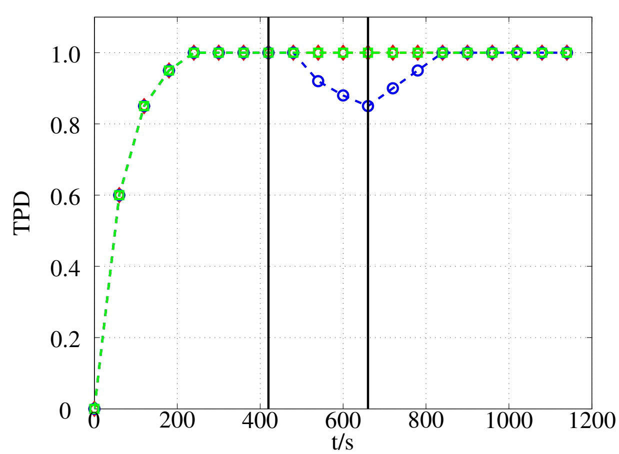

Fig. 13: Track probability of detection of targets in Scenario 2. Turn from 420 s to 640 s. TEK (red, diamonds), TMK (blue, circles), TAT (green, squares)